ICSV14
Cairns • Australia
9-12 July, 2007

STRONG COUPLING OF THE FAST MULTILEVEL MULTIPOLE BOUNDARY ELEMENT METHOD WITH THE FINITE ELEMENT METHOD FOR VIBRO–ACOUSTIC PROBLEMS

Dominik Brunner, Michael Junge, Lothar Gaul

Institute of Applied and Experimental Mechanics
University of Stuttgart
70550 Stuttgart, Germany

brunner@iam.uni-stuttgart.de

Abstract

Nowadays, the sound quality has an ever-growing influence on the overall impression of a product. To predict the sound radiation of structures, both a structural and an acoustic problem have to be solved. In this work, the structural part is modelled by the finite element (FE) method, whereas the exterior acoustic problem is efficiently simulated with the boundary element (BE) method . To overcome the well known bottleneck of fully populated boundary element matrices, the fast multilevel multipole method is applied. In case of thin structures and dense fluids, a strong coupling between the two problems is essential, since the effect of the acoustic pressure onto the surface of the structure is not negligible. Two different methods are investigated: First, the structural displacements are eliminated yielding a Schur complement formulation. Secondly, the problem is formulated with a Lagrangian multiplier and an Uzawa-type algorithm with nested inner-outer iterations is applied. In both cases, iterative solvers with different preconditioners are used.

1. INTRODUCTION

In the structural-acoustic simulations presented here, a strong coupling between fluid and structure is taken into account. For the structural part, the FE method turned out to be well suited for engineering applications. In most cases, a FE/FE coupling scheme is applied if interior acoustic problems are investigated [1]. In contrast, a FE/BE coupling approach is superior for exterior problems, since the Sommerfeld radiation condition is automatically fulfilled [3]. An optimal efficiency is obtained by accelerating the BE part with the fast multilevel multipole method. Two different FE/fast BE coupling schemes are investigated in this paper. First, the theory of the different approaches is discussed. Then, the coupling algorithms are considered. Finally, two numerical examples are investigated.

2. FUNDAMENTALS

The structural vibrations are simulated by the finite element method, whereas the exterior acoustic problem is efficiently modelled by the boundary element method. Below, the characteristic equations for the structure and the fluid are derived in the frequency domain. Throughout this paper the time-harmonic behavior $\mathrm{e}^{-\mathrm{i}\,\omega\,t}$ will by applied, where i is the imaginary number, $\omega = 2\,\pi\,f$ denotes the angular frequency and f is the excitation frequency. The normal vector $n(x)$ on the coupling interface Γ_{int} is defined to point into the fluid.

2.1. Structural Fundamentals

The structural part is assumed to be linear elastic. A weak form of the equation of motion is obtained by applying d'Alembert's principle [1]

$$\delta\mathbf{u}^{\mathrm{T}} \underbrace{\int_{\Omega} \mathbf{B}^{\mathrm{T}}\mathbf{C}\,\mathbf{B}\,\mathrm{d}\Omega}_{\mathbf{K}_{\mathrm{s}}}\,\mathbf{u} = -\delta\mathbf{u}^{\mathrm{T}}\,\underbrace{\rho\int_{\Omega}\mathbf{N}_u^{\mathrm{T}}\mathbf{N}_u\,\mathrm{d}\Omega}_{\mathbf{M}_{\mathrm{s}}}\,\frac{\mathrm{d}^2}{\mathrm{d}t^2}\mathbf{u} + \delta\mathbf{u}^{\mathrm{T}}\underbrace{\int_{\Gamma_p} -\mathbf{N}_u^{*\mathrm{T}} n\,\mathbf{N}_p\,\mathrm{d}\Gamma}_{-\mathbf{C}_{\mathrm{FE}}}\,\mathbf{p} + \delta\mathbf{u}^{\mathrm{T}}\mathbf{f}_{\mathrm{s}}, \qquad (1)$$

where $\mathbf{B}$ is the strain-displacement matrix and $\mathbf{C}$ is the elasticity matrix with the strain-stress relationship. The nodal displacement, pressure, and force vector are given by $\mathbf{u}$, $\mathbf{p}$ and $\mathbf{f}_s$ and $\mathbf{N}_u$ and $\mathbf{N}_p$ are the matrices with the shape functions for the displacement and pressure, respectively. In case of $\mathbf{N}_u^*$ rotational degrees of freedom are neglected. The mass and stiffness matrices are denoted by $\mathbf{M}_{\mathrm{s}}$ and $\mathbf{K}_{\mathrm{s}}$, respectively. The coupling matrix $\mathbf{C}_{\mathrm{FE}}$ takes into account the effect of an acoustic pressure onto the structure. Equation (1) must be fulfilled for an arbitrary virtual displacement $\delta\mathbf{u}^{\mathrm{T}}$. Transformation to the frequency domain and introduction of a Rayleigh damping yields the system of equations

$$\underbrace{\left(-\omega^2\mathbf{M}_{\mathrm{s}} - \mathrm{i}\omega\mathbf{D}_{\mathrm{s}} + \mathbf{K}_{\mathrm{s}}\right)}_{\mathbf{K}_{\mathrm{FE}}}\mathbf{u} + \mathbf{C}_{\mathrm{FE}}\,\mathbf{p} = \mathbf{f}_s. \qquad (2)$$

The damping matrix is assumed to be a linear combination of the mass and stiffness matrix $\mathbf{D}_{\mathrm{s}} = \alpha\,\mathbf{M}_{\mathrm{s}} + \beta\,\mathbf{K}_{\mathrm{s}}$. To obtain a flexible simulation tool, $\mathbf{M}_{\mathrm{s}}$ and $\mathbf{K}_{\mathrm{s}}$ are directly imported from the commercial FE package ANSYS.

2.2. Fluid Fundamentals

In the following, the exterior acoustic problem is considered. Starting point of the fluid formulation is the time-harmonic Helmholtz equation

$$\nabla^2 p(x) + \kappa^2\,p(x) = 0, \qquad (3)$$

which is valid for the pressure p at an arbitrary point x within the exterior acoustic domain Ω_e. The circular wavenumber is denoted by $\kappa = \frac{\omega}{c}$, where c is the sound velocity of the acoustic fluid. A weak form of the Helmholtz equation can be obtained by weighing with the fundamental solution $P^* = \frac{\mathrm{e}^{\mathrm{i}\kappa\,r}}{4\,\pi\,r}$, where r denotes the distance between source and field point. Applying Green's second theorem yields the representation formula which is valid for a field point within the acoustic domain. The boundary integral equation can be obtained by shifting the field point

onto the smooth boundary

$$\frac{1}{2}\,p(x) = -\underbrace{\int_\Gamma P^*(x,y)\,q(y)\,\mathrm{d}s_y}_{(Vq)(x)} + \underbrace{\int_\Gamma \frac{\partial P^*(x,y)}{\partial n_y}\,p(y)\,\mathrm{d}s_y}_{(Kp)(x)}, \quad x \in \Gamma, \tag{4}$$

with the acoustic flux $q(x) = \frac{\partial p(x)}{\partial n}$. The single layer potential is denoted by V and the double layer potential by K, respectively. Analogously, the hypersingular boundary integral equation is derived by an additional derivative with respect to the normal

$$\frac{1}{2}q(x) = -\underbrace{\int_\Gamma \frac{\partial P^*(x,y)}{\partial n_x}\,q(y)\,\mathrm{d}s_y}_{(K'q)(x)} + \underbrace{\int_\Gamma \frac{\partial^2 P^*(x,y)}{\partial n_x \partial n_y}\,p(y)\,\mathrm{d}s_y}_{-(Dp)(x)}, \quad x \in \Gamma, \tag{5}$$

where K' denotes the adjoint double layer potential and D is the hypersingular operator.
A Galerkin formulation can be obtained by testing these equations on the coupling interface Γ_{int}. Introducing shape functions for $p(x)$ and $q(x)$ results in an algebraic system of equations. Further details on the BE formulation are given in section 3 and 4.
A serious drawback of classical BE methods is, that setting up the fully populated BE matrices is of order $\mathcal{O}(N^2)$, where N denotes the number of degrees of freedom. To overcome this bottleneck, the fast multilevel multipole method is applied.

2.2.1. Fast Multilevel Multipole Boundary Element Method

In order to use the multipole method, all elements are grouped by means of clusters. In contrast to classical BE formulations, which compute the effect of every source point onto every field point, the sources of every cluster are first summed up, transformed to the other clusters and finally distributed to the field points. Typically, one has to evaluate potentials of the type

$$\Phi(x_b) = \sum_{a=1}^{A} \frac{\mathrm{e}^{\mathrm{i}\kappa|x_b - y_a|}}{|x_b - y_a|} q_a, \tag{6}$$

where q_a denotes the source strength and $|x_b - y_a|$ is the distance between the source and field point. This distance can be split up into three portions: First, the distance $|z_a - y_a|$ between the source point and the center of the source cluster. Secondly, D which only depends on the distance between the centers of the two clusters and finally $|x_b - z_b|$, that is local to the field point cluster. Using these distances, the potential can be rewritten by means of the diagonal multipole expansion [2]

$$\Phi(x_b) = \frac{\mathrm{i}\kappa}{4\pi} \int_{S^2} \mathrm{e}^{\mathrm{i}\kappa(x_b - z_b)\cdot s} M_L(s,D) \underbrace{\sum_{a=1}^{A} \mathrm{e}^{\mathrm{i}\kappa(z_a - y_a)\cdot s} q_a}_{F(s)}\,\mathrm{d}s. \tag{7}$$

The sum in (7) is called "farfield signature" $F(s)$. The translation operators $M_L(s, D)$ are defined by

$$M_L(s, D) = \sum_{\ell=0}^{L} (2\ell + 1)\mathrm{i}^{\ell} h_{\ell}^{(1)}(\kappa|D|) P_{\ell}(s \cdot \hat{D}) \tag{8}$$

with the Hankel functions h_ℓ and the Legendre polynoms P_ℓ. Since the multipole expansion is only valid for well separated source and fieldpoints, one has to split up the clusters into a near- and farfield. The nearfield is represented by a sparse matrix. It has to be evaluated by classical BEM. To obtain an optimal efficiency, a multilevel cluster tree is used. This fast multilevel multipole (FMM) algorithm has a quasi linear complexity of order $\mathcal{O}(N \log^2 N)$. For a detailed description the reader is referred to [4].

3. DIRECT COUPLING WITH BURTON-MILLER FORMULATION

The first coupling procedure uses a Burton-Miller formulation for the BE part. Motivated by the fact, that neither the boundary (4) nor the hypersingular boundary integral equation (5) has an unique solution for an exterior acoustic problem, a linear combination of both is applied, which is known as the Burton-Miller approach

$$\left(-\frac{1}{2}I + K\right) p(x) + \frac{\mathrm{i}}{\kappa}(Dp)(x) = (V\, q)(x) + \frac{\mathrm{i}}{\kappa}\left(-\frac{1}{2}I - K'\right) q(x). \tag{9}$$

Testing (9) with linear test functions yields a Galerkin formulation. The flux on the coupling interface is now expressed by the structural displacements in normal direction

$$q(x) = \rho_{\mathrm{f}}\, \omega^2 u(x) \cdot n(x), \tag{10}$$

where ρ_{f} is the density of the fluid. Introducing a triangulation of the boundary and interpolating the pressure and displacement with the shape functions φ^p and φ^u leads to the algebraic system of equations

$$\underbrace{\left(-\frac{1}{2}\mathbf{I} + \mathbf{K} + \frac{\mathrm{i}}{\kappa}\mathbf{D}\right)}_{\mathbf{K}_{\mathrm{BE}}} \mathbf{p} \underbrace{-\rho_{\mathrm{f}}\, \omega^2 \left(\mathbf{V} - \frac{\mathrm{i}}{2\kappa}\mathbf{I}' - \frac{\mathrm{i}}{\kappa}\mathbf{K}'\right)}_{\mathbf{C}_{\mathrm{BE}}} \mathbf{u} = 0. \tag{11}$$

By combining (2) and (11), the coupled system including the FE part is formally written as

$$\underbrace{\begin{pmatrix} \mathbf{K}_{\mathrm{FE}} & \mathbf{C}_{\mathrm{FE}} \\ \mathbf{C}_{\mathrm{BE}} & \mathbf{K}_{\mathrm{BE}} \end{pmatrix}}_{\mathbf{K}} \begin{pmatrix} \mathbf{u} \\ \mathbf{p} \end{pmatrix} = \begin{pmatrix} \mathbf{f}_{\mathrm{s}} \\ 0 \end{pmatrix}. \tag{12}$$

Since a direct solver would cause an expense of order $\mathcal{O}(N^3)$ in case of fully populated matrices, an iterative GMRES solver is used for the coupled system (12).

3.1. Iterative GMRES Solver with Preconditioning

By introducing the Schur complement $\mathbf{S} = \mathbf{K}_{\text{BE}} - \mathbf{C}_{\text{BE}}\mathbf{K}_{\text{FE}}^{-1}\mathbf{C}_{\text{FE}}$, the exact solution of the coupled system can be written as

$$\mathbf{p} = -\mathbf{S}^{-1}\mathbf{C}_{\text{BE}}\mathbf{K}_{\text{FE}}^{-1}\mathbf{f}_{\text{s}} \qquad \text{and} \qquad \mathbf{u} = \mathbf{K}_{\text{FE}}^{-1}(\mathbf{f}_{\text{s}} - \mathbf{C}_{\text{FE}}\mathbf{p}). \tag{13}$$

Two different solvers are investigated:

1. The fully coupled system (12) is solved by a single GMRES solver ("full"-solver). Since **p** and **u** are of totally different magnitudes when using SI units, a nondimensionalization is performed. Additionally, a block diagonal preconditioner is constructed with the approximate inverses of $\mathbf{K}_{\text{FE}}$ and $\mathbf{K}_{\text{BE}}$. Incomplete LU (ILU) and LU factorizations are used for this purpose.
2. The reduced system on **p** (13 left) is solved by a single GMRES solver ("reduced"-solver). In this case, a nondimensionalization is implicitly included in the formulation and does not have to be performed manually. The exact inverse $\mathbf{K}_{\text{FE}}^{-1}$ in the Schur complement is needed at every iteration step. It can efficiently be computed by a direct solver, using a factorization, e.g. a LU-solver. This factorization is then applied at every iteration step. A preconditioner can be constructed by approximating the inverse of the Schur complement by $\mathbf{K}_{\text{BE}}^{-1}$. An ILU and an approximate inverse preconditioner (AIP) are compared. The structural displacements **u** are computed in a postprocessing step with (13 right).

4. COUPLING FORMULATION WITH LAGRANGE MULTIPLIERS

In this section an alternative coupling formulation is discussed. The pressure on the coupling interface Γ_{int} is chosen as Lagrange multiplier, i.e. $\lambda = p_{\text{int}}$ [3]. In contrast to the formulation before, the boundary integral equation (4) is tested with constant test functions ν^q and the additional term $\int_{\Gamma_{\text{int}}} \nu^q \left(p^{\text{int}} - \lambda\right) \mathrm{d}\Gamma_x$ is introduced to enforce the equilibrium condition. The hypersingular boundary integral equation (5) is tested with linear test functions ν^p on the same boundary. The continuity condition between structural displacement and flux is formulated in the weak sense by

$$\int_{\Gamma_{\text{int}}} \nu^\lambda \left(-\rho_{\text{f}}\omega^2 u_n + q^{\text{int}}\right) \mathrm{d}\Gamma_x = 0. \tag{14}$$

The pressure p_{int} is interpolated by linear shape functions and constant shape functions are used for the flux q. Taking into account the FE part (2) leads to the algebraic system of equations

$$\left(\begin{array}{c|c|c|c} \rho_{\text{f}}\,\omega^2\mathbf{K}_{\text{FE}} & & & \mathbf{C}_{\text{FE}} \\ \hline & -\tilde{\mathbf{V}} & \frac{1}{2}\tilde{\mathbf{I}} + \tilde{\mathbf{K}} & -\tilde{\mathbf{C}}_{\text{BE}} \\ \hline & -\frac{1}{2}\tilde{\mathbf{I}}^{\text{T}} - \tilde{\mathbf{K}}^{\text{T}} & -\tilde{\mathbf{D}} & \\ \hline -\mathbf{C}_{\text{FE}}^{\text{T}} & \tilde{\mathbf{C}}_{\text{BE}}^{\text{T}} & & \end{array}\right) \left(\begin{array}{c} \mathbf{u} \\ \mathbf{q}_{\text{int}} \\ \mathbf{p}_{\text{int}} \\ \boldsymbol{\lambda} \end{array}\right) = \left(\begin{array}{c} \rho_{\text{f}}\,\omega^2\mathbf{f}_{\text{s}} \\ 0 \\ 0 \\ 0 \end{array}\right). \tag{15}$$

In contrast to the previous formulation, the coupling matrix $\tilde{\mathbf{C}}_{\text{BE}}$, which arises from the continuity condition (14), is sparse now.

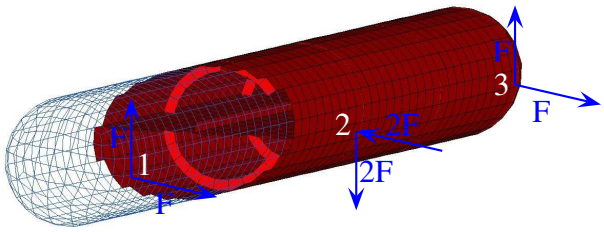

Figure 1. Submarine-like structure.

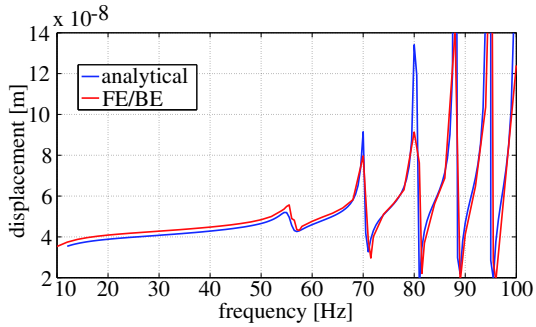

Figure 2. Sphere: FE/BE- vs. analytical solution.

4.1. Uzawa Algorithm

The use of an iterative solver on the system (15) shows poor convergence. Therefore, an Uzawa algorithm is used to introduce a reduced system which is solved for the Lagrange multiplier λ ("Lagrange-solver")

$$\left[\mathbf{C}_{\mathrm{FE}}^{\mathrm{T}}\left(\rho_{\mathrm{f}}\omega^2\mathbf{K}_{\mathrm{FE}}\right)^{-1}\mathbf{C}_{\mathrm{FE}}+\tilde{\mathbf{C}}_{\mathrm{BE}}^{\mathrm{T}}\tilde{\mathbf{K}}_{\mathrm{BE}}^{-1}\tilde{\mathbf{C}}_{\mathrm{BE}}\right]\boldsymbol{\lambda}=\mathbf{C}_{\mathrm{FE}}^{\mathrm{T}}\left(\rho_{\mathrm{f}}\omega^2\mathbf{K}_{\mathrm{FE}}\right)^{-1}\rho_{\mathrm{f}}\omega^2\,\mathbf{f}_{\mathrm{s}}. \tag{16}$$

The inner inverse $\left(\rho_{\mathrm{f}}\omega^2\mathbf{K}_{\mathrm{FE}}\right)^{-1}$ of (16) is computed by a direct LU solver. A GMRES is used to evaluate $\tilde{\mathbf{K}}_{\mathrm{BE}}^{-1}$, which stands for the BE part. The matrix-vector product can efficiently be computed by the FMM algorithm. Two different preconditioners are investigated to approximate $\tilde{\mathbf{K}}_{\mathrm{BE}}^{-1}$: A diagonal scaling and an incomplete LU factorization (ILU). A GMRES without preconditioning is applied for the outer iterations. The structural displacements can finally be computed in a postprocessing step.

5. NUMERICAL RESULTS

The efficiency in terms of computation time and memory consumption is investigated by means of a sphere and a submarine-like structure (Fig. 1).

5.1. Spherical Shell Structure

The first problem is a spherical shell structure driven by a harmonic point force of 10 N at the north pole. The structure has a diameter of 10 m and a shell thickness of 5 cm. It is built of steel with a Young's modulus of 207 GPa and a Poisson's ratio of 0.3. The sphere is totally submerged in water. For this type of problem, an analytical series solution is available [5]. Figure 2 compares the FE/BE solution with the analytical solution. The structure is discretized by 2600 SHELL63 elements of triangular shape. Both, the direct coupling formulation and the Lagrange formulation show nearly the same results so that the two graphs coincide. Both solutions show a low deviation from the analytical solution. There is a strong influence of the coupling, as the first three uncoupled structural eigenfrequencies are at 122 Hz, 144 Hz and 152 Hz. Obviously, the hydromass effect shifts the resonances significantly to smaller frequencies demonstrating the necessity of a strong coupling scheme.

In both formulations, the most time consuming part is the evaluation of the BE matrix-

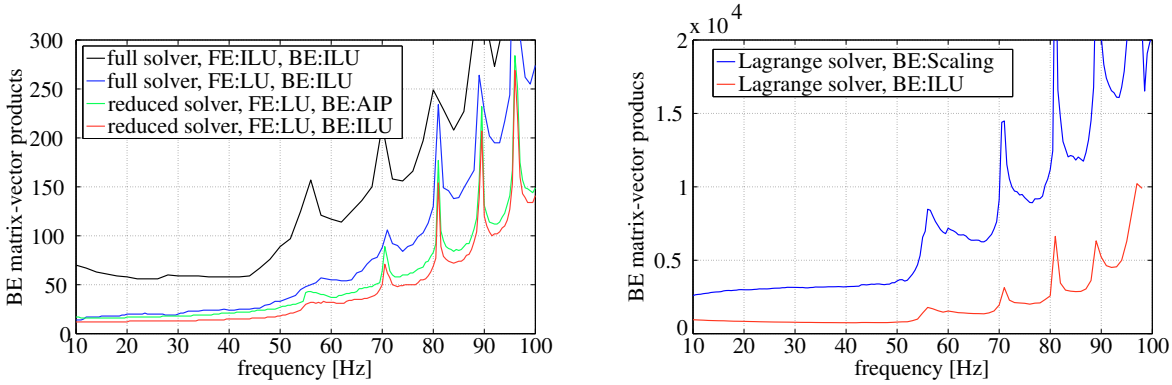

Figure 3. Spherical shell structure (1334 elements): Number of BE matrix-vector evaluations of the direct coupling formulations (left) and of the Lagrange coupling formulation (right) for different preconditioners.

vector product by means of the FMM algorithm. Therefore, the number of evaluated products is compared for both formulations with different preconditioners. Figure 3 shows the number of matrix-vector evaluations for the direct coupling formulation (left) and the Lagrange formulation (right). The most efficient solver is a combination of a direct LU solver for the FE part and an ILU preconditioned GMRES working on the reduced system. The use of an AIP instead of an ILU shows a similar performance. Due to the nested inner-outer iteration scheme of the Lagrange formulation, the number of matrix-vector products is significantly larger. One has to mention, that a GMRES without any preconditioning was used for the outer loop. Additionally, the efficiency could by improved by applying an inexact Uzawa algorithm [3].

Concerning the memory consumption, the two formulations mainly differ in their nearfields. In case of the Lagrange solver, the memory consumption for the nearfield is 45 MB compared to 31 MB in case of the direct formulation. The reason is, that it is more expensive to store $\tilde{\mathbf{V}}$ and $(\frac{1}{2}\tilde{\mathbf{I}} + \tilde{\mathbf{K}})$ of the Lagrange scheme (15) than $\mathbf{C}_{\mathrm{BE}}$ of the direct formulation (12). The two remaining matrices $\tilde{\mathbf{D}}$ and $\mathbf{K}_{\mathrm{BE}}$ have the same memory consumption.

5.2. Submarine-Like Structure

In order to show that the direct coupling formulation can efficiently simulate large scale problems, a second structure is investigated. The structure (Fig. 1) consists of a 20 m long cylinder with a diameter of 2 m and spherical caps on both sides. Stiffeners are mounted every 2 m along the center-line. An intermediate bottom is additionally included in the model. The shell thickness is 2cm and the material data as mentioned above are applied. In this case, a Raleigh damping with α=50 $\frac{1}{\mathrm{s}}$ and β=1e-6 s is included in the simulation. The structure is discretisized with 10,600 SHELL63 elements of quadrilateral shape. The structure is excited by six harmonic point forces.

Figure 4 (left) shows the results of frequency sweeps of the pure FE solution and coupled FE/BE solutions with and without Rayleigh damping. Due to the hydromass effect there is a significant shift of the resonance frequencies. If damping is considered, the resonances in the frequency range between 50 and 100 Hz almost disappear. The right plot shows the necessary BE matrix-vector product evaluations when the direct coupling algorithm on the reduced system is applied with a ILU preconditioner. The approach shows a good convergence with less than 60 evaluations over a wide range. Due to the high efficiency and low memory consumption, even frequency sweeps with 200 individual frequency steps can be computed without difficulty.

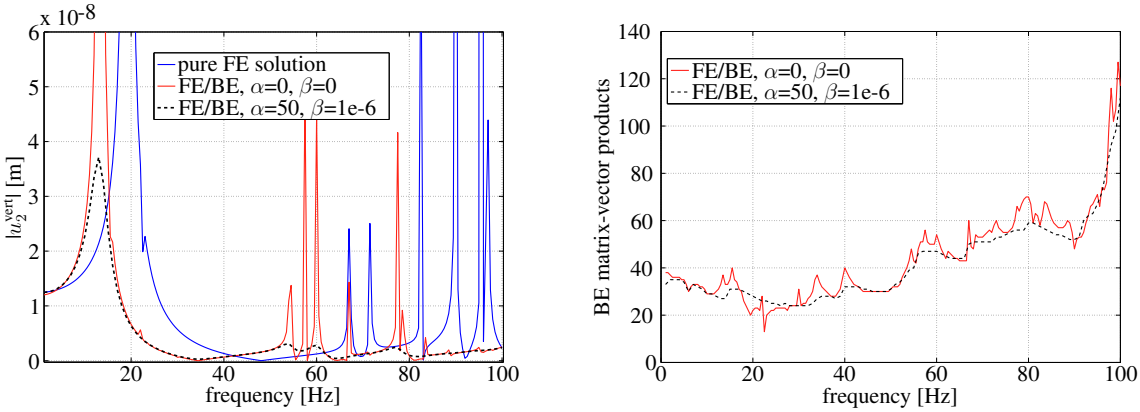

Figure 4. Submarine-like structure: Frequency response at node 2 in vertical direction (left) and number of iterations for the direct coupling scheme with the reduced system(right).

In contrast to this, the number of necessary matrix-vector evaluations in case of the Lagrange formulation would be too high to run these frequency sweeps with the Lagrange coupling formulation on a standard business PC within a reasonable amount of time.

6. CONCLUSION

The investigations show, that both coupling formulations show a good accuracy compared to an analytical solution. Both formulations are studied with different preconditioners which turn out to have a significant influence on the convergence behavior. In terms of efficiency, the direct coupling formulation appears to be superior on the Lagrange formulation for the examined model problem. Due to the low number of iterations and the applications of the fast multipole boundary element method, even problems with more than 100,000 dofs can be simulated. Concerning the memory consumption, the direct coupling formulation is more advantageous. The simulation tool turns out to be well suited to solve typical engineering problems, since the finite element matrices are imported from the commercial FE package ANSYS.

Acknowledgement

Financial support for this research project, granted by the German Research Foundation through the transfer project SFB404/T3, is gratefully acknowledged.

REFERENCES

[1] Zienkiewicz, O.C. and Taylor, R.L., *The Finite Element Method*. Butterworth-Heinemann, Oxford, 2000.

[2] Rokhlin, V.: “Diagonal forms of translation operators for the Helmholtz equation in three dimensions”, *Applied and Computational Harmonic Analysis* **1**, 82-93(1993).

[3] Fischer, M: *The Fast Multipole Boundary Element Method and its Application to Structure-Acoustic Field Interaction*. PhD-thesis, Institute of Applied and Experimental Mechanics, Stuttgart University, 2004.

[4] L. Gaul, M. Fischer, “Large-scale simulations of acoustic-structure interaction using the fast multipole BEM”, *ZAMM* **86**, 4-17(2006).

[5] Junger, C; Feit D.: *Sound, structures, and their interaction*. MIT Press, Cambridge, 1972.